



ISSN: 0067-2904

## Structural and dielectric properties of Zr doped BaTiO<sub>3</sub> synthesized by microwave assisted chemical route

Muthafar F. Al-Hilli

Department of Physics, College of Science, University of Baghdad, Baghdad, Iraq.

### Abstract

Lead-free ferroelectric nano ceramics of BaZr<sub>x</sub>Ti<sub>1-x</sub>O<sub>3</sub> (x=0.1, 0.2 and 0.3) were prepared by means of microwave assisted chemical route. The structural, dielectric and electrical properties were examined. The crystalline structure of the specimens was studied by X-ray diffraction patterns. All the samples showed pure single phase of perovskite structure with space group of I4/mcm. X-ray diffraction data illustrated that there is no secondary phases exist. Structural and electrical properties of barium titanate ceramics are influenced significantly by small additions of Zr. The electrical conductivity showed higher values at x=0.2 and decreased at higher Zr content. The Hall charge mobility is found to decrease with Zr addition. The negative sign of the Hall coefficient R<sub>H</sub> confirms the dominant n-type conduction in all samples. The charge carrier concentration decreased with Zr content increase. Suggested potential application for this ceramics compound is in high storage multilayer capacitors and ferroelectric applications.

**Keywords:** Piezoelectrics, perovskite, chemical route

## الخواص التركيبية والعزلية لتطعيم BaTiO<sub>3</sub> بمادة Zr والمصنعة بواسطة الطريقة الكيميائية المساعدة باستخدام المايكروويف

مظفر فؤاد جميل الحلي

قسم الفيزياء، كلية العلوم، جامعة بغداد، بغداد، العراق.

### الخلاصة

المركب السيراميكي النانوي BaZr<sub>x</sub>Ti<sub>1-x</sub>O<sub>3</sub> حيث ان (x=0.1, 0.2 and 0.3) تم تحضيره بالطريقة الكيميائية المساعدة باستخدام المايكروويف. تم دراسة الخصائص التركيبية والعزلية والكهربائية. تركيب البنية البلورية للعينات درست باستخدام حيود الاشعة السينية. جميع العينات المحضرة اظهر تركيبها وجود طور احادي من البيروفسكايت ينتمي للمجموعة الفضائية I4/mcm. حيود الاشعة السينية اظهرت عدم وجود اطوار ثانوية في التركيب. تبين ان الخصائص التركيبية والبنوية والكهربائية تتأثر بشكل كبير بأضافة صغيرة من Zr. التوصيلية الكهربائية اظهرت عند اعلى قيمة عند اضافة مقدارها x=0.2 وتبدأ بالانخفاض عند قيم الاضافة الاعلى. وجد بأن قيم تحركية هول للشحنات تنخفض مع اضافة Zr. الاشارة السالبة لمعامل هول تبين ان ميكانيكة التوصيل السائدة هي من النوع السالب لجميع العينات. تبين ان تركيز حاملات الشحنة يتناقص مع زيادة تركيز اضافة Zr. من التطبيقات المقترحة لهذا المركب هي في المتسعات متعددة الطبقات ذات الخزن العالي وفي التطبيقات الفيروكهربائية.

## 1. Introduction

Piezoelectric compounds are distinguished by the ability of transforming the energy from electrical into mechanical, and vice versa. However, bulk piezoelectrics suffer from several disadvantages; accordingly composite piezoelectric compounds are the best technological option for most of applications. Nowadays, due to miniaturization of the piezoelectric composite materials and the utilization of PZT fibers in place of piezoelectric bars, new applications for sensors and actuators became potentially feasible [1]. Ba[Ti<sub>(1-x)</sub>Zr<sub>x</sub>]O<sub>3</sub> (BZT) solid solution was attracted much interest because of its distinguished dielectric properties for many application such as capacitors, actuators and sensors [2].

Most of the significant piezoelectric materials are found in the form of perovskite crystalline structure. The perovskite unit cell is cubic possesses a large size cation located at the cell corners (for example, Ba<sup>+2</sup> or Pb<sup>+2</sup>), and a smaller cation located in the unit cell body center (for example, Ti<sup>+4</sup> or Zr<sup>+4</sup>) and the face centered sites of the unit cell are occupied by the oxygen anions. The structure of crystal is built up of a network of corner linked oxygen octahedra, with the smaller cation occupying the octahedral holes sites [3].

Many factors, like dopant type, porosity, impurities, and grain size, play a role in the characteristics of piezo materials. Their characteristics are basically temperature dependant and deteriorate just beneath the Curie temperature. The elastic and dielectric constants are sensitive to the change in crystal structure [4]. Donor-doping BaTiO<sub>3</sub> solid solutions with ions (e.g., Ca<sup>2+</sup>, Sr<sup>2+</sup>, La<sup>3+</sup>, Zr<sup>4+</sup> and Nb<sup>5+</sup>, etc.) were and still subject to intensive investigations for their diverse applications and motivating ferroelectric and dielectric behaviors. Especially, compositionally modified BaZr<sub>x</sub>Ti<sub>1-x</sub>O<sub>3</sub> (BZT) attends much attention because of the tunable microstructure and electrical characteristics towards specific applications, because of Zr<sup>4+</sup> (atomic weight of 91.2 atomic radius of 86 pm) is with chemical stability much higher than Ti<sup>4+</sup> (atomic weight of 47.9, ionic radius of 74.5 pm). The rise in zirconium content in piezoelectric materials, especially for content  $x > 0.25$ , leads to vast dielectric peaks showing frequency dispersion, i.e., ferroelectric-relaxation behavior [5, 6].

In this work, nano powder of BaTiO<sub>3</sub> was prepared by chemical route. The structural, dielectric, Hall effect as well as AC and DC conductivity properties of the BaZr<sub>x</sub>Ti<sub>1-x</sub>O<sub>3</sub> ( $x = 0.1, 0.2$  and  $0.3$ ) as a function of zirconium content, frequency and temperature were examined.

## 2. Experimental

BaZr<sub>x</sub>Ti<sub>1-x</sub>O<sub>3</sub> nano ceramics with  $x=0.1, 0.2$  and  $0.3$  were prepared by microwave assisted chemical route. Precursor solution of BZT was prepared from barium acetate, zirconium n-propoxide, and titanium isopropoxide. Barium acetate with the required stoichiometric amount to produce the correct values of  $x= 0.1, 0.2$  and  $0.3$  was dissolved in acetic acid at temperature of 70°C through continuous stirring. To ensure complete dissolution of barium acetate in acetic acid ethylene glycol was added gradually to the solution. Solid KOH was then added gradually to bring the pH to 11. Stoichiometric amount of zirconium n-propoxide (C<sub>12</sub>H<sub>32</sub>O<sub>4</sub>Zr), and titanium isopropoxide (C<sub>12</sub>H<sub>32</sub>O<sub>4</sub>Ti) were added and microwave assisted refluxing was turned on. The system operated at a frequency of 2.45 GHz and could operate at 100 % full irradiation power of 850 W. The reactions were carried out in Teflon vessels at 90 °C for 90 min. After then, the solid powder was separated from solutions by centrifugation and were thoroughly washed for three times using deionized distilled water, and then dried inside an oven at 70°C. The samples were prepared by pressing at 2 MPa to produce pellet samples with diameter of 15mm and thickness of 3 mm. The specimens were fired at 1100 °C for 3 h in atmospheric furnace environment and cooled down to ambient. The formation of the desired compound was examined by X-ray diffraction technique which was performed on XRD-6000 Shimadzu Japan diffractometer with Cu K $\alpha$  radiation ( $\lambda= 1.540598 \text{ \AA}$ ), at scan speed= 5.0 deg/min. The topology of the samples was investigated by using the AFM. The dielectric measurements and DC conductivity and polarization were carried out at (296 - 493 K) and frequency range (100 Hz- 10 MHz) using 4274A and 4275A Multi-Frequency LCR Meter HEWLETT-PACKARD. The Hall effect measurements were carried out by four- point probe technique on Ecopia HMS-3000 at room temperature. The samples apparent density and porosity were measured accurately by the hydrostatic method using Archimedes principle [7].

### 3. Results and discussion

Figure-1 shows the XRD patterns of the ceramic system  $\text{Ba}(\text{Zr}_x\text{Ti}_{1-x})\text{O}_3$  where  $x=0.1, 0.2$  and  $0.3$ . It may be noticed that all the samples showed pure single phase with a tetragonal perovskite structure of the space group of  $I4/mcm$ . This suggests that Zr addition diffuses into the  $\text{BaTiO}_3$  lattice to produce a solid solution. Moreover, the diffraction peaks were seen to shift towards low angle with increasing Zr content. Because the radius of  $\text{Zr}^{4+}$  ions ( $0.86 \text{ \AA}$ ) is greater than the size of  $\text{Ti}^{4+}$  ( $0.75 \text{ \AA}$ ), subsequently, the replacement of  $\text{Ti}^{4+}$  with  $\text{Zr}^{4+}$  may results in the expansion of the lattice parameter of perovskite ceramic compound [8]. A weak peaks belonging to the tetragonal perovskite crystal structure phase were detected at low sintering temperature ( $1100 \text{ }^\circ\text{C}$ ). This indicates a poor crystallinity of the nano  $\text{Ba}(\text{Zr}_x\text{Ti}_{1-x})\text{O}_3$  ceramics in the peaks of (110), (111), (120) and (121) directions. At Zr addition of  $x=0.2$ , the diffraction peaks were very well defined and the growth of peaks of (110), (111) and (121)-oriented grains was noted. The density results of the prepared compound are shown in tables 1. The density was found to increase with Zr content increase ranging between 93-96 % of the theoretical density of the ceramic system  $\text{Ba}(\text{Zr}_x\text{Ti}_{1-x})\text{O}_3$ .

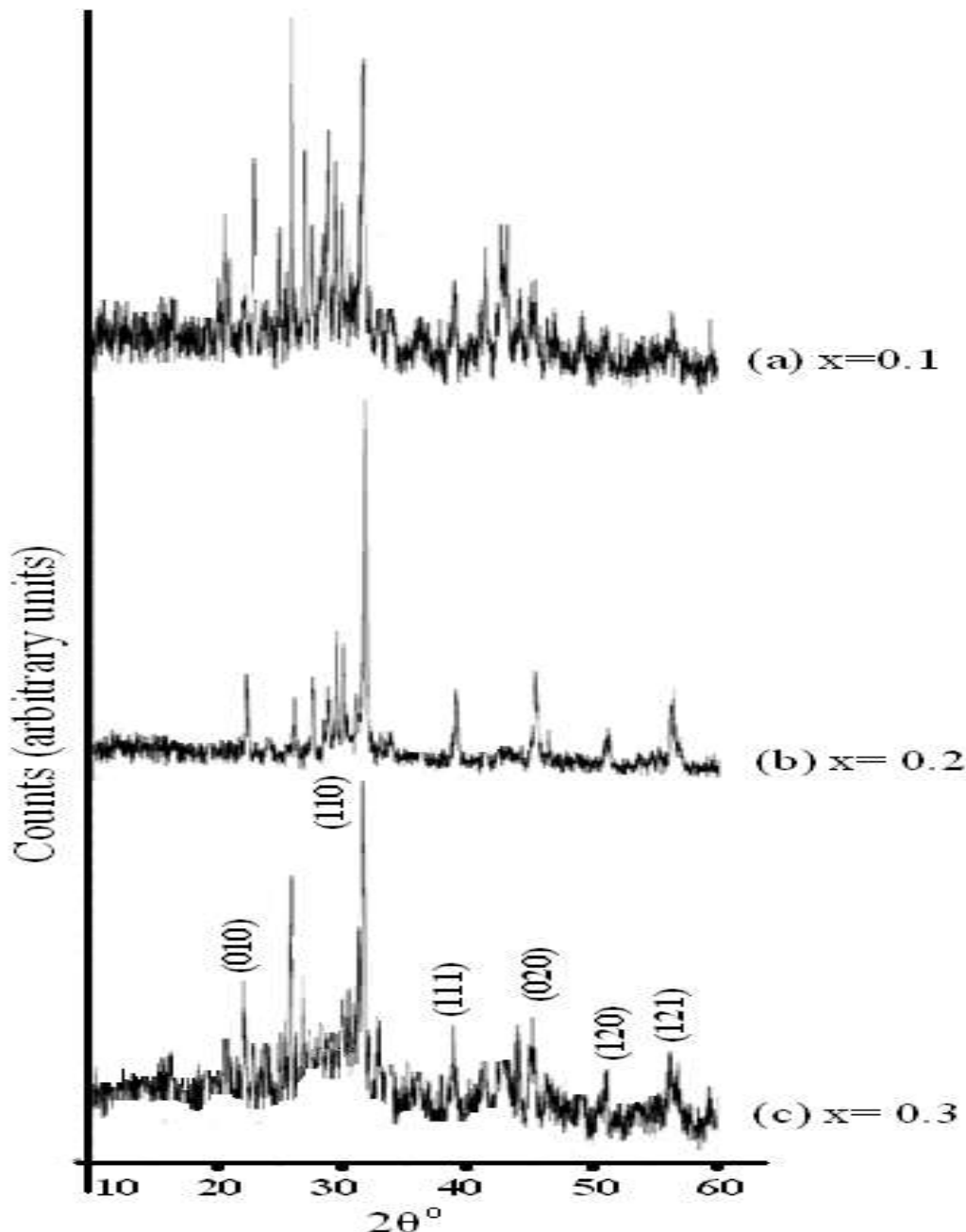
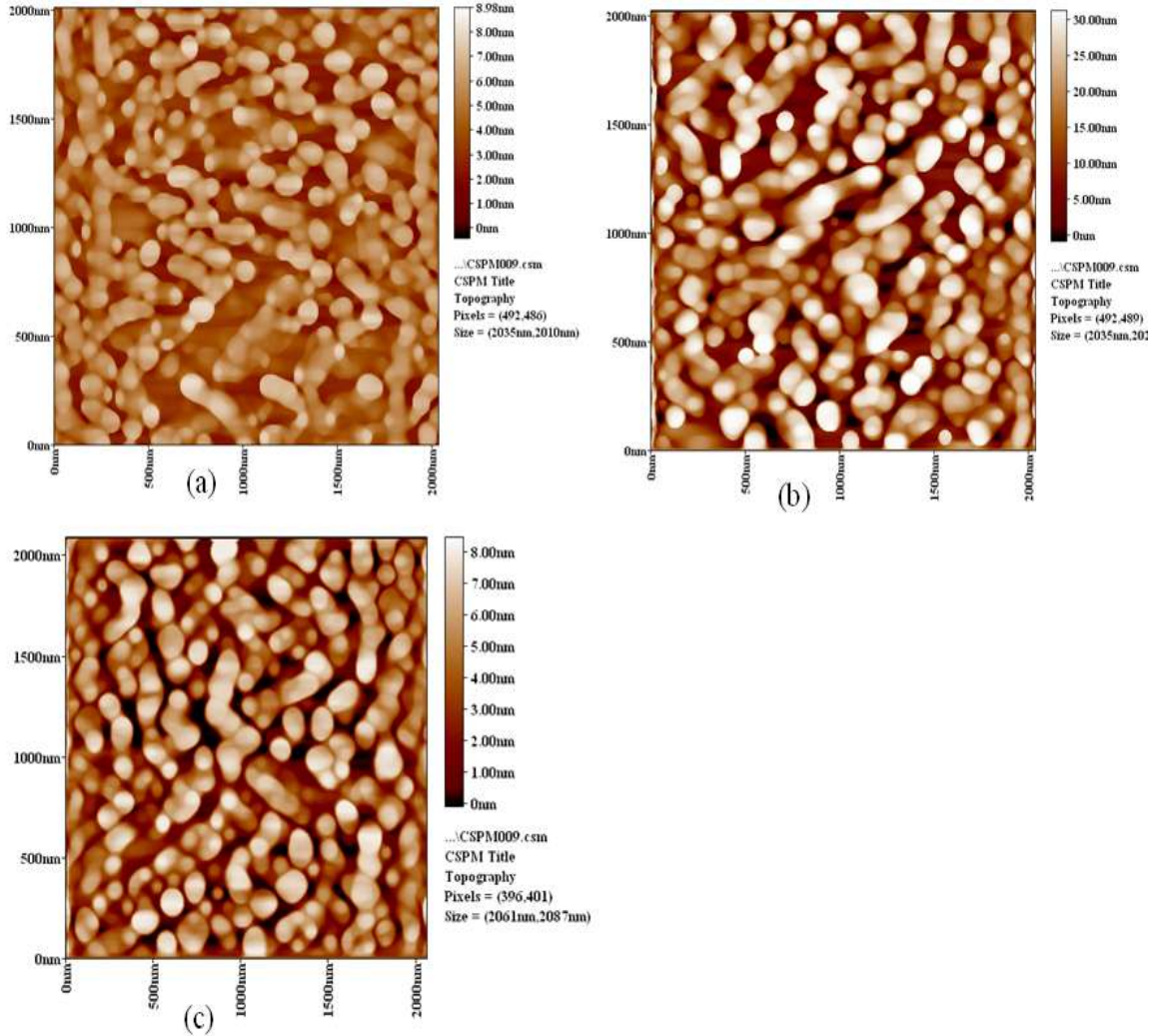


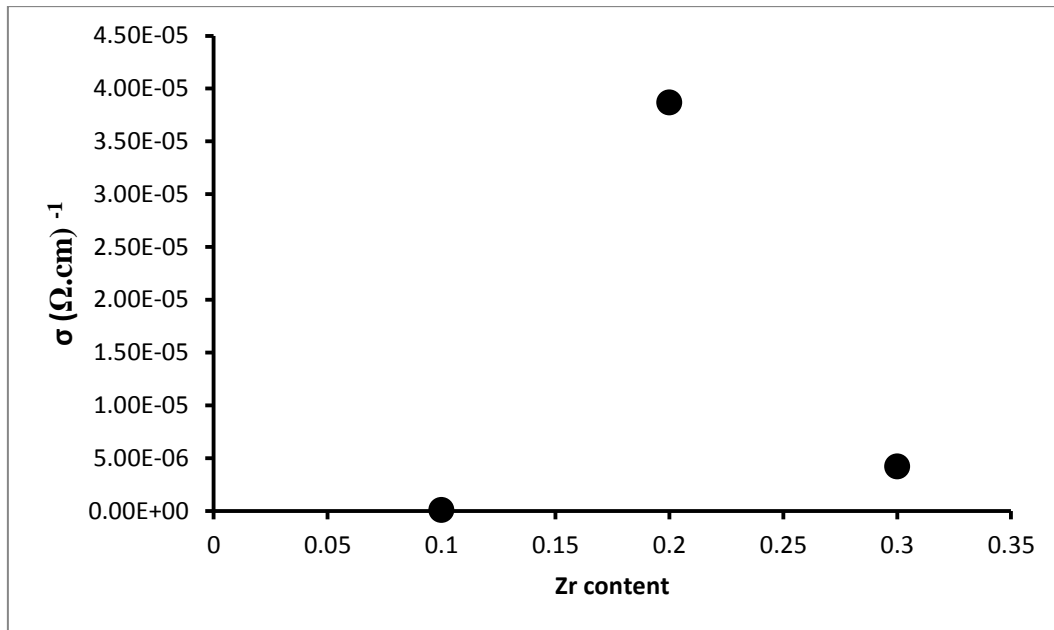
Figure1- XRD patterns of  $\text{Ba}(\text{Zr}_x\text{Ti}_{1-x})\text{O}_3$  samples.

The surface morphological characteristics of samples were examined by using atomic force microscopically imaging as shown in Figure-2. The surface topology of Ba (Zr<sub>x</sub>Ti<sub>1-x</sub>)O<sub>3</sub> ceramics is homogeneous with existence of some evident pores located at the grain boundary. The microstructure of specimen with x=0.1 shown in Figure-2(a), is basically homogeneous and no pores are found at the grain boundary, while the average grain size is about 69.32 nm. The microstructure of the sample with x=0.2 Figure- 2(b), is also homogeneous and few pores may be noticed at the grain boundary with average grain size of about 81.08 nm. For the sample with x=0.3 Figure-2(c), a higher proportion of porosity could be seen at the grain boundary and the average grain size is about 71.23 nm.



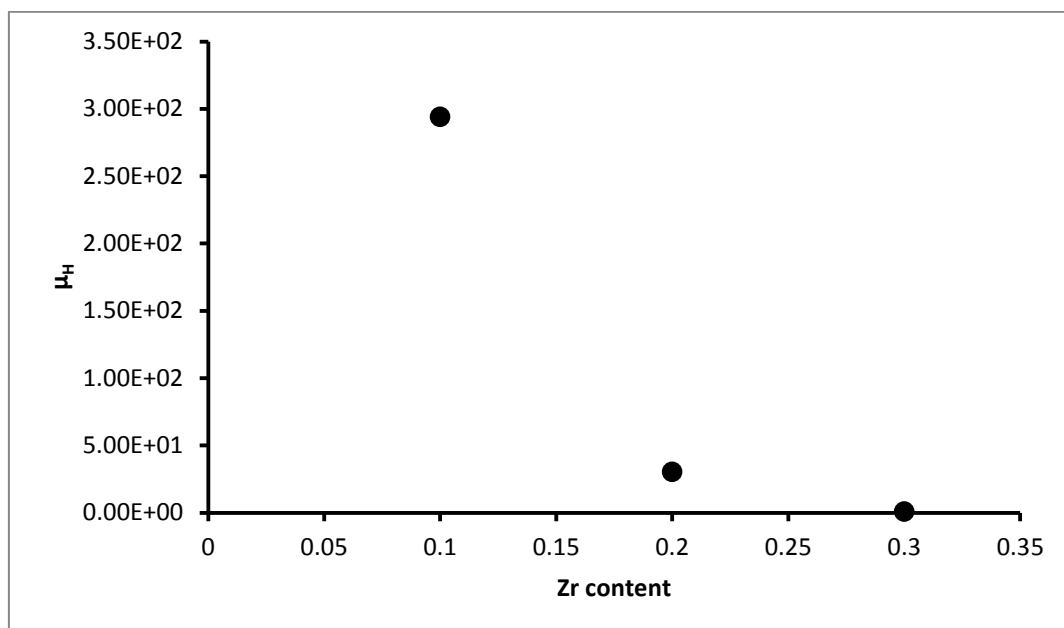
**Figure 2-** AFM photographs of BaZr<sub>x</sub>Ti<sub>1-x</sub>O<sub>3</sub> , (a) x=0.1, (b) x= 0.2 and (c) x= 0.3.

Figure-3 shows the relationship of the DC electrical conductivity versus the Zr content. The conductivity showed higher values at x=0.2 and decreased at higher Zr addition. The higher conductivity region occurs when the electronic compensation mechanism dominates, beyond a critical concentration of donor, the mechanism of cation vacancies compensation becomes dominant and electrical conductivity falls down as it's seen for the addition x=0.3. This is because of the increase in charge concentration and the generation of oxygen vacancies due to the oxygen loss during the sintering process as proposed by Voisin et al. [9]. The compensation of charge according to the reaction (Kröger and Vinks)  $O_o \rightarrow \frac{1}{2} O_2 \uparrow + V_o'' + 2e^-$ , which may creates free electron making the ceramic n-type [10]. When Zr ion occupies Ba-sites, Ti<sup>4+</sup> could be reduced to Ti<sup>3+</sup> and formed a conduction electron (Ti<sup>4+</sup>•e) which keeps charge neutrality. Subsequently, the resistivity of nano ceramic was decreased sharply [11].



**Figure 3-**DC electrical conductivity of BaZr<sub>x</sub>Ti<sub>1-x</sub>O<sub>3</sub> (x=0.1, 0.2 and 0.3).

The Hall mobility dependence on the Zr content for BaZr<sub>x</sub>Ti<sub>1-x</sub>O<sub>3</sub> is shown in Figure-4. The Hall mobility is found to decrease with Zr addition. In table 1 it is seen that the negative sign of the Hall coefficient  $R_H$  confirms the dominant *n*-type conduction behavior in all samples in agreement with the behavior described by Kolodiazhnyi et al. [12]. The charge concentration decreased with Zr content increase as given in Table 1. This may be attributed to the fact that Zr<sup>2+</sup> and Zr<sup>4+</sup> are more reducible than the Ti<sup>4+</sup>; thus the electrons were trapped at these sites. Eventually, the hopping motion of the trapped electrons from one Zr ionic site to another was almost prohibited. This means that the conduction charge carriers were effectively localized at these Zr sites. This in turn resulted in a decrease of charges carrier concentration, in agreement with the observations of Wanga et al. [13]. The magneto-resistance given by the Hall effect measurement results are given in Table-1. The positive magneto-resistance was found to decrease with Zr content.



**Figure 4-**Variation of Hall mobility with Zr content for BaZr<sub>x</sub>Ti<sub>1-x</sub>O<sub>3</sub>.

**Table 1-**The change in Average grain size, charge concentration, resistivity, magneto-resistance and Hall coefficient with Zr content.

Zr content(x)	Average grain size (nm)	Apparent density ( $\text{g}/\text{cm}^3$ )	Relative Density %	Charge concentration ( $\text{n}/\text{cm}^2$ )	$\rho$ ( $\Omega\cdot\text{cm}$ )	Magneto-resistance ( $\Omega$ )	Hall coefficient $R_H$ ( $\text{m}^2/\text{C}$ )
0.1	69.32	5.62	93.33	-2.40E+09	1.54E+08	7.43E+06	-1.83E+09
0.2	81.08	5.71	94.83	-6.87E+11	2.53E+04	2.30E+04	-9.55E+05
0.3	71.23	5.79	96.16	-7.78E+12	9.25E+09	4.27E+04	-1.17E+05

Figure-5 illustrates the AC conductivity versus frequency at different Zr content. At low frequencies region the AC conductivity is flattened. This may be attributed to the DC conductivity behavior of the material. The AC conductivity of the specimens was found to increase markedly with frequency rise. The large conductivity at higher frequency region is most likely due to the hopping motion of ions from one preferable site to the other [14]. Hopping mechanism conduction is dominant in ionic lattice in which, cations of the same kind exists in two oxidation states. In small polaron model, the AC conductivity increases with the increase of frequency as proposed by Mahajan et al. [15]. When the Zr addition is increased, the number of electron hopping sites may be increased thereby increasing the conductivity. This increase in AC conductivity may also be ascribed to the increase in grain sizes with Zr content increase [16].

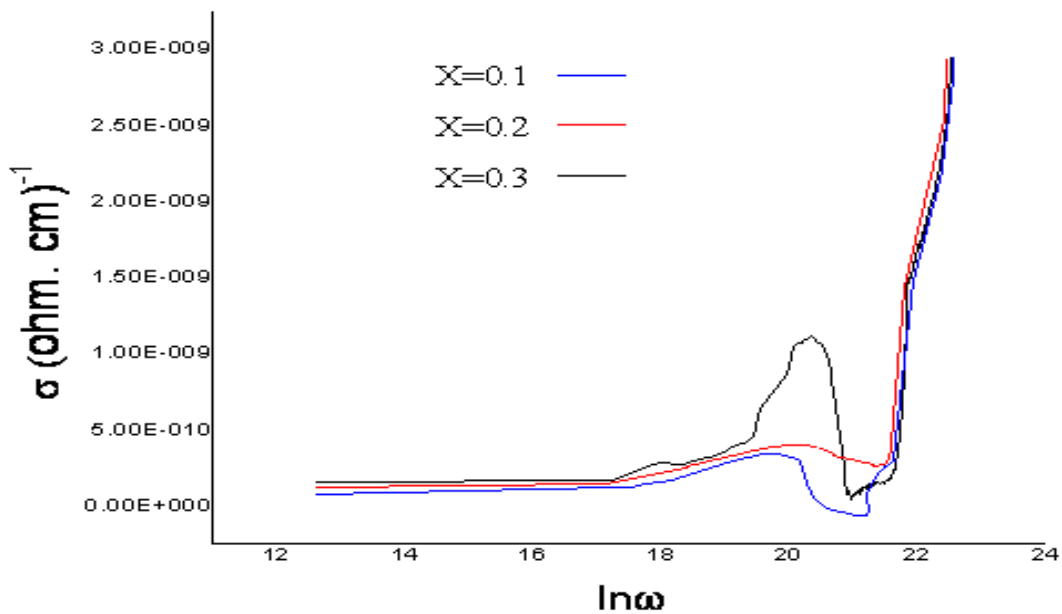
**Figure 5-** AC conductivity versus  $\ln \omega$  of  $\text{BaZr}_x\text{Ti}_{1-x}\text{O}_3$ ,  $x=0.1, 0.2$  and  $0.3$ .

Figure-6 shows the change in dielectric constant with frequency at different Zr concentrations. The dielectric constant was found to increase with Zr content. The high of  $\epsilon'$  ( $\epsilon_r = \epsilon'/\epsilon_0$ ) at lower frequencies may be ascribed to the effect of multi component mechanisms of polarization (namely, space charge, orientation, ionic and electronic). Since, when higher frequencies applied the dipoles become unable oscillate quickly enough, causing the dipoles oscillations to lag behind that of the applied field. When the frequency is raised the dipole becomes entirely incapable to keep up with the applied field, therefore the orientation component of polarization freezes. This would cause a fall off in the dielectric constant and attains a steady value at higher frequencies which mainly results from the interfacial polarization [17]. The dielectric constant increased at higher values of Zr addition. This could be ascribed to the growing in the size of grains, because the dielectric constant of the material is linearly proportional to the average value of its grain size [18]. Figure-7 illustrates the relationship of the dielectric loss factor with the frequency. At low frequencies region, the dielectric loss showed higher values. This may be attributed to the existence of non-uniform charge piling up at the grain boundaries. Two mechanisms are accompanied along with the dielectric loss. First mechanism is

resistive loss and another one is relaxation loss. In case of resistive dielectric loss, the mobile charge carriers consume the energy in the ceramic material. In the later, i.e. relaxation loss mechanisms, the dissipation of energy is mainly due to relaxation of dipoles. Figure-8 shows the dielectric loss tangent ( $\tan\delta = \epsilon''/\epsilon'$ ) versus frequency for different Zr addition level. It may be noticed that the loss tangent (dielectric loss) obeys a decreasing tendency with increase in zirconium content. At high frequency region, dielectric loss becomes independent of the frequency showing a platform behavior [16, 19].

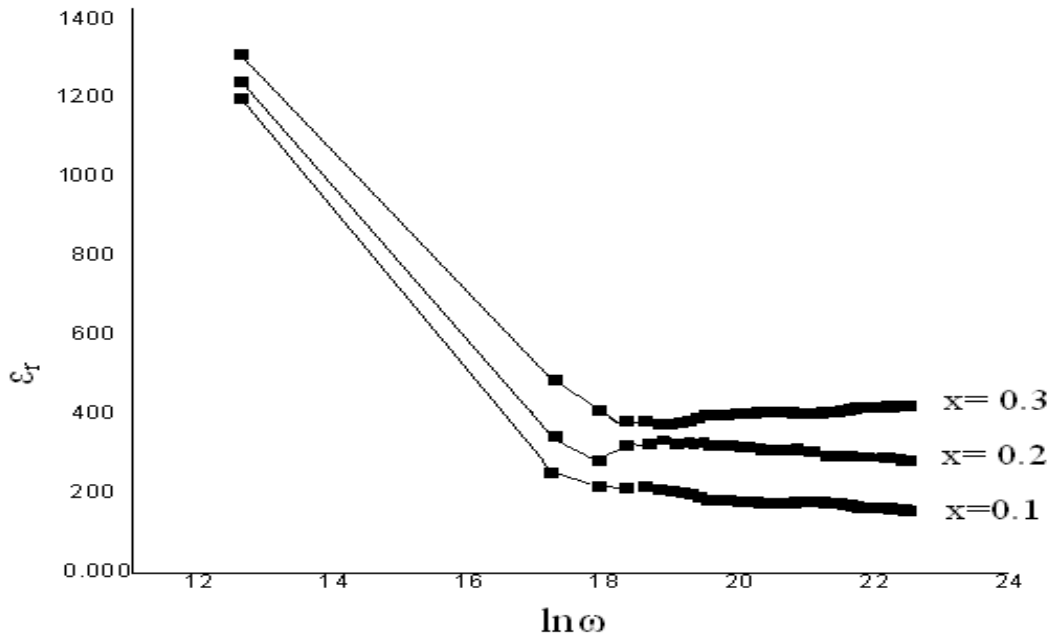


Figure 6- relative dielectric constant versus  $\ln \omega$  of  $BaZr_xTi_{1-x}O_3$ ,  $x=0.1, 0.2$  and  $0.3$

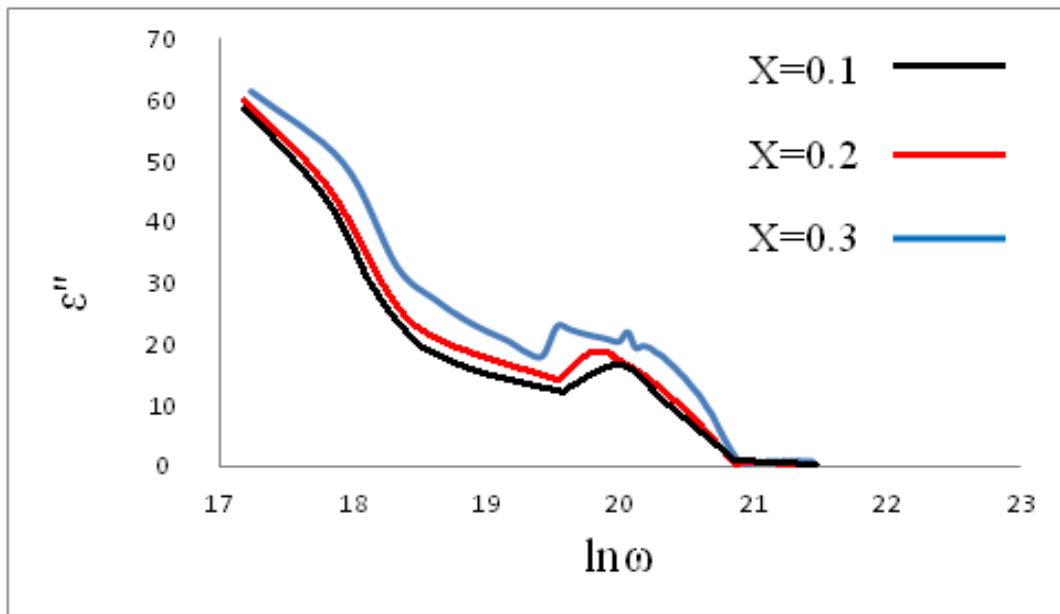
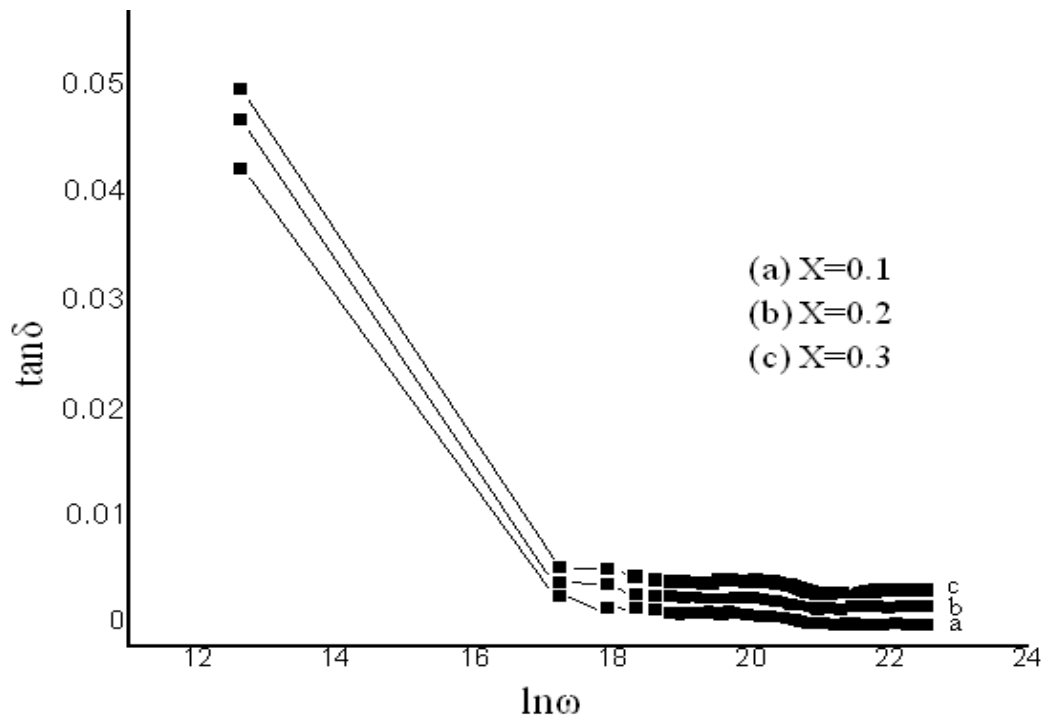


Figure7- dielectric loss versus  $\ln \omega$  of  $BaZr_xTi_{1-x}O_3$ ,  $x=0.1, 0.2$  and  $0.3$



**Figure 8-** dielectric loss tangent versus  $\ln \omega$  of  $\text{BaZr}_x\text{Ti}_{1-x}\text{O}_3$ ,  $x=0.1, 0.2$  and  $0.3$ .

#### 4. Conclusion

The  $\text{BaZr}_x\text{Ti}_{1-x}\text{O}_3$  nano ceramic system where  $x=0.1, 0.2$  and  $0.3$  were prepared by microwave assisted chemical route. The formation of single phase perovskite structure was confirmed. This preparation technique could results in a grain size for the prepared nano ceramic compound ranged between 70-80 nm (well below 100 nm). Microwave assisted synthesis route could substantially reduces the sintering temperature and soaking time. Density of the compact of about 96 % of theoretical density was attained by this preparation technique. The conductivity showed a significant dependence upon the addition of Zr to  $\text{BaTiO}_3$  and exhibited higher value at  $x=0.2$  then decreased at higher Zr addition. The prepared ceramic compound showed n-type conductivity behavior proposing and electron hopping conduction mechanism. The conductivity behavior demonstrated charge carrier dependence. The dielectric results showed higher dielectric constant with low dielectric loss. The lead free  $\text{BaTiO}_3$  compound doped with Zr is an environmentally friendly ceramic compound, which makes it an excellent candidate for various applications. Piezoelectric  $\text{BaZr}_x\text{Ti}_{1-x}\text{O}_3$  ceramics compound one of the most promising materials for dielectric and ferroelectric applications.

#### References

1. Harald Berger, Sreedhar Kari, Ulrich Gabbert, Reinaldo Rodriguez-Ramos, Julian Bravo-Castillero, Raúl Guinovart-Diaz, **2005**. Calculation of effective coefficients for piezoelectric fiber composites based on a general numerical homogenization technique. *Composite Structures*, **71**: 397–400.
2. Moura, F., Simões, A.Z., Paskocimas, C.A., Zaghete, M.A., Varela, J.A. and Longo, E. **2010**. Temperature dependence on the electrical properties of  $\text{Ba}(\text{Ti}_{0.90}\text{Zr}_{0.10})\text{O}_3$ : 2V Ceramics. *Materials Chemistry and Physics* **123**: 772–775.
3. Michael, W. Lufaso and Patrick M. Woodward, **2001**. Prediction of the crystal structures of perovskites using the software program SPuDS, *Acta Cryst.* **B57**: 725-738
4. Sridhar, S., Giannakopoulos, A.E., Suresh, S. and Ramamurty, U. **1999**. Electrical response during indentation of piezoelectric materials: A new method for material characterization. *journal of applied physics*, **85**(1): 380-387.
5. Wei Li, Zhijun Xu, Ruiqing Chu, Peng Fu, and Guozhong Zang, **2010**. Dielectric and piezoelectric properties of  $\text{Ba}(\text{Zr}_x\text{Ti}_{1-x})\text{O}_3$  lead-free ceramics. *Brazilian Journal of Physics*, **40**(3): 353-356.
6. Dixit, A., ajumder, S.B., Savvinov, A., Katiyar, R.S., Guo, R., Bhalla, A.S. **2002**. Investigations on the sol–gel-derived barium zirconium titanate thin films. *Materials Letters*, **56**: 933– 940.

7. Johanna Engstrand Unosson, Cecilia Persson, Hakan Engqvist, **2015**. An evaluation of methods to determine the porosity of calcium phosphate cements. *Journal of biomedical materials research b: applied biomaterials*, **103 B**(1): 62-71.
8. Rashmi Chourasia, O.P. Shrivastava, **2011**. Crystal structure modeling, electrical and microstructural characterization of manganese doped barium zirconium titanate ceramics. *Polyhedron*, **30**: 738–745.
9. Christophe Voisin, Sophie Guillemet-Fritsch, Pascal Dufour, and Christophe Tenailleau, **2013**. Influence of Oxygen Substoichiometry on the Dielectric Properties of BaTiO<sub>3</sub>-d Nanoceramics Obtained by Spark Plasma Sintering. *International Journal of Applied Ceramic Technology*, **1-2**. pp. 2-12. DOI:10.1111/ijac.12058.
10. Lily, K., Kumari, K., Prasad and Choudhary, R.N.P. **2008**. Impedance analysis of (Na<sub>0.5</sub>Bi<sub>0.5</sub>)(Zr<sub>0.25</sub>Ti<sub>0.75</sub>)O<sub>3</sub> ceramic. *Indian journal of engineering and materials sciences*, **15**: 147-151.
11. Shamima Choudhury, Shurayya Akter, Rahman, M.J., Bhuiyan, A.H., Rahman, S.N., Khatun, N. and Hossain, M.T. **2008**. Structural, Dielectric and Electrical Properties of Zirconium Doped Barium Titanate Perovskite. *Journal of Bangladesh Academy Of Sciences*, **32**(2): 221-229.
12. Kolodiazny, T., Petric, A., Niewczas, M., Bridges, C., Safa-Sefat A. and Greedan, J.E. Thermoelectric power, **2003**. Hall effect, and mobility of *n*-type BaTiO<sub>3</sub>. *Physical Review B* **68**, 085205, 1-5, DOI: 10.1103/PhysRevB.68.085205.
13. Xiang Wang, Min Gua, Bin Yanga, Shining Zhua, Wenwu Cao, **2003**. Hall effect and dielectric properties of Mn-doped barium titanate. *Microelectronic Engineering*, **66**: 855–859.
14. Kumar, P., Chandra, Ajit R., Kulkarni, Priyanka, Kamal Prasad, **2017**. Structure and electrical properties of Ba (In<sub>0.5</sub>Nb<sub>0.5</sub>)<sub>1-x</sub>Ti<sub>x</sub>O<sub>3</sub> ceramics. *Processing and Application of Ceramics*, **11**(3): 191–200.
15. Mahajan, R.P., Patankar, K.K., Kothale, M.B. and Patil, S.A. **2000**. Conductivity, dielectric behaviour and magnetoelectric effect in copper ferrite–barium titanate composites. *Bull. Mater. Sci.*, **23**(4): 273–279.
16. H.Hemanta Singh, A. Deepak Sharma and H. Basantakumar Sharma, **2017**. Dielectric and Electrical Properties of Barium Zirconate Titanate Ceramics. *International Journal of Engineering Technology, Management and Applied Sciences*, **5**(3): 178-184.
17. Enyew Amare Zereffa and Alamanda Vara Prasadarao. **2012**. Effect of Zirconium Substitution on the Electrical Properties of Ferroelectric (Bi<sub>0.5</sub>Na<sub>0.5</sub>)<sub>0.94</sub>Ba<sub>0.06</sub>TiO<sub>3</sub> Ceramics. *International Research Journal of Pure & Applied Chemistry*, **2**(2): 130-143.
18. Priyambada Nayak, Tanmaya Badapanda, Anil Kumar Singh and Simanchalo Panigrahi, **2017**. An approach for correlating the structural and electrical properties of Zr<sup>4+</sup>-modified SrBi<sub>4</sub>Ti<sub>4</sub>O<sub>15</sub>/SBT ceramic. *RSC Adv.*, **7**: 16319–16331.
19. Pathan A.T. and Shaikh, A.M. **2012**. Dielectric Properties of Co-Substituted Li-Ni-Zn Nanostructured Ferrites Prepared Through Chemical Route. *International Journal of Computer Applications*, **45**(21): 0975 – 8887.